Coupling MATSim and the PALM Model System Large Scale Traffic and Emission Modelling with High Resolution Computational Fluid Dynamics Dispersion Modelling

Janek Laudan[a,1,*], Sabine Banzhaf[b], Basit Khan[c], Kai Nagel[a]

[a] *Technische Universität Berlin, Kaiserin-Augusta-Allee 104-106, 10553, Berlin, Germany*
[b] *Freie Universität Berlin , Carl-Heinrich Becker-Weg 6-10, 12165, Berlin, Germany*
[c] *Mubadala Arabian Center for Climate and Environmental Sciences (ACCESS), New York University Abu Dhabi, Abu Dhabi, United Arab Emirates*

Abstract

To effectively mitigate anthropogenic air pollution, it is imperative to implement strategies aimed at reducing emissions from traffic-related sources. Achieving this objective can be facilitated by employing modeling techniques to elucidate the intricate interplay between environmental impacts and traffic activities.

This paper highlights the importance of combining traffic emission models with chemistry transport models in urban areas at street canyon level and presents the development and implementation of an interface between the mesoscopic traffic and emission model MATSim and PALM-4U, which is a set of urban climate application modules within the PALM model system. The proposed coupling mechanism converts MATSim output emissions into input emission flows for the PALM-4U chemistry module, which requires translating between the differing data models of both modelling systems. In particular, temporal resolution, spatial representation, and file formats must be transformed to establish an interface between both models.

The presented coupling mechanism provides a novel technique for accurate traffic emissions and dispersion in urban areas at ultra-high resolution. The interface is tested in an idealized case study focused on identifying "Hot Spots" of pollutant concentrations and pollution exposure, caused by simulated traffic in the Berlin city, demonstrating the potential for improving air quality assessment and management in urban areas.

Keywords: Traffic Simulation, Emission Modelling, Air Pollution, Pollution Hot Spot, CFD

1. Introduction

In light of the burgeoning urbanization trend, with over half of the global population presently dwelling in urban areas (Desa, 2018), the concern regarding air pollution has intensified significantly. Prolonged exposure to air pollution can lead to adverse effects on diverse physiological systems, encompassing the respiratory, cardiovascular, metabolic, and neurological functions (Schulz et al., 2018). Despite a decline in premature deaths in Europe, air pollution remains a significant health concern (Ciarelli et al., 2019; European Environment Agency, 2020).

One of the main sources of urban air pollution in cities is car traffic, as shown by studies measuring individual exposure (Dons et al., 2011; Lim et al., 2021) or by applying statistical methods (McConnell et al., 2010). In addition, Ehrnsperger and Klemm (2022) and von Schneidemesser et al. (2021) find that pollutant concentrations correspond to observed traffic patterns in urban environments, making reduction

*Corresponding author
Email addresses: laudan@tu-berlin.de (Janek Laudan), banzhaf@zedat.fu-berlin.de (Sabine Banzhaf), basit.khan@nyu.edu (Basit Khan), nagel@vsp.tu-berlin.de (Kai Nagel)

of traffic-induced emissions a priority to mitigate pollutant concentrations and improve the health situation of the urban population.

Developing mitigation strategies for the impact of traffic emissions requires understanding the relation between traffic and its environmental impact. The first step in modelling this relation is to compute emissions from traffic using an emission model. Forehead and Huynh (2018), Mądziel (2023) and Ma et al. (2012) provide a comprehensive overview of available traffic emission models, which can be divided into two categories:

1. **Aggregate** traffic emissions are based on aggregated parameters such as: Average vehicle speed on links or overall vehicle distance travelled. Important models are for example: MOBILE6 (Agency, 2002), MOVES (Epa, 2021), COPERT (Ntziachristos, 2000) or ARTEMIS (André et al., 2008)
2. **Microscopic** emitted pollution is calculated at the vehicle level, considering attributes such as vehicle speed, acceleration, engine type and others. Prominent models are CMEM (Scora and Barth, 2006), VT-MICRO (Rakha et al., 2004), EMIT (Cappiello et al., 2002) and POLY (Qi et al., 2004)

Aggregate and microscopic emission models are best combined with different categories of traffic models as input for emission calculations. Aggregate models work well with aggregate traffic models while microscopic emission models require input on the vehicle level which requires the use of micro- or mesoscopic traffic models (Forehead and Huynh, 2018; Ma et al., 2012).

Once traffic emissions are properly modelled, a dispersion model can be used to investigate the dispersion of pollution in the urban environment. Johnson (2022) provides an introduction into dispersion models in general, while Vardoulakis et al. (2003) and Forehead and Huynh (2018) list traffic related dispersion models. These include Line-Source-Models such as CALINE (Benson, 1992), RLINE (Snyder et al., 2013) as well as operational models such as OSPM (Berkowicz et al., 1997), ADMS (Carruthers et al., 1994), or IMMIS (Diegmann, 2011) which parameterize turbulence in street canyons and even include atmospheric chemistry reactions.

More accurate results are to be expected from CFD (Computational Fluid Dynamics) models of which, in addition to the reviews above, Tominaga and Stathopoulos (2016) and Khan et al. (2021) provide an overview of models capable of simulating emission dispersion. In contrast to parameterized models, CFD models are based on atmospheric turbulent fluid dynamics, solving differential equations to determine atmospheric pressure and flow within discrete raster cells of the simulated domain (Wendt, 2008, p. 87). By simulating atmospheric turbulence and solving a transport equation together with a model driven, chemical mechanism, the pollutant concentrations and dispersion can be calculated (Liang et al., 2023). For emission calculations, either RANS (Reynolds-Averaged-Navier-Stokes) or LES (Large Eddy Simulation) models are used, of which LES requires more computational resources but can provide more accurate results regarding wind flow around obstacles like buildings (Blocken, 2018).

Several studies have applied traffic induced emissions with dispersion models. Forehead and Huynh (2018) includes a list of applications where most of the studies use aggregate emission and parameterized dispersion models (e.g., Batterman et al. (2015)), or simulate small domains using microscopic emission and dispersion models (e.g., Grumert et al. (2015)). Liang et al. (2023) provides a more recent overview of coupling CFD dispersion and traffic emission models. They find that *"CFD models are generally used for pollutant dispersion studies at the street or micro-district level* (Liang et al., 2023) due to the requirements on computational resources. In contrast to the majority of studies, Sanchez et al. (2017) and San José et al. (2021) have presented high-resolution emission dispersion calculation in real urban environments. Both studies use high-resolution traffic models to calculate traffic emissions and CFD-RANS models for dispersion simulation.

Adding to the cited work, this paper describes the development of an interface between the mesoscopic traffic and emission model MATSim (Multi Agent Transport Simulation) (Horni et al., 2016) and the urban climate simulation model PALM-4U (Maronga et al., 2020) which was developed as part of the UC^2 (Urban Climate Under Change) (UC2, 2023) project. MATSim simulates traffic dynamics across large regions, accommodating millions of simulated persons. Employing a mesoscopic approach, MATSim captures individual vehicles without explicitly modelling vehicle dynamics such as acceleration or following behavior, which enables the calculation of traffic induces emissions for large urban areas. PALM-4U, a CFD model which is designed to be scaled onto HPC (High Performance Computing) infrastructure, is able to simulate chemical transformation, advection, and deposition of air pollutants for large realistically shaped urban areas (Maronga et al., 2020). By operating in LES mode, it provides an accurate representation of atmospheric turbulence, especially in urban canopies with complex building geometries. The implemented interface is tested by conducting an idealized case study which investigates pollutant concentrations caused by simulated traffic in the area of Berlin, focusing on the identification of *Hot Spots* areas where pollutant concentrations are particularly high.

2. Technical prerequisites

The proposed coupling mechanism is built on top of existing technology, which is described in the following section.

2.1. Traffic simulation

MATSim is an open-source traffic simulation which models travelers as individual simulated persons (Horni et al., 2016). Each simulated person maintains a daily plan of activities which it tries to accomplish throughout the day. To reach activities of their plan, simulated persons travel along a simulated road network, competing for limited resources with other simulated persons. Each simulated person tries to maximize its utility by adapting to the limited traffic supply. The optimization of utility is done in the form of a co-evolutionary algorithm where the same day is iterated multiple times. One iteration includes three steps:

1. During the mobility simulation, simulated persons execute their individual plans while interacting with other simulated persons. To support large-scale scenarios, vehicles are simulated using a queue model, omitting calculation of computationally complex vehicle dynamics or car following behavior. However, the queue model accounts for congestion and spill back effects important for mesoscopic traffic patterns.
2. The executed plan of each simulated person is evaluated through a utility score. In general, performing activities increases the score, spending time in traffic or monetary costs, e.g., public transit fares or cost of car ownership decrease the score.
3. A fraction of all simulated persons adapt their behavior by inventing new plans. This includes choosing alternative routes, switching between modes or adapting departure times. The remaining share of simulated persons picks a plan from the set of plans that it has already memorized.

After a certain number of iterations, the simulation reaches an equilibrium where individual simulated persons cannot improve their situation any further.

2.2. Emission model

The MATSim framework provides an extension for emission modelling, initially developed by Hülsmann et al. (2011) and later improved by Kickhöfer et al. (2013). Based on the simulated traffic dynamics, emissions are calculated using emission factors from the HBEFA (Handbook Emission Factors for Road Transport) version 4.1 database (Notter et al., 2019), which accounts for traffic situations such as road type, current traffic flow and vehicle speed, as well as vehicle properties such as vehicle type and engine type being the most important. Emissions in MATSim are calculated on a per-link basis. This corresponds to the level of detail at which traffic is simulated. Once a vehicle has traversed a link in the network, corresponding emission factors are selected from the HBEFA database. The emission factors for different pollutants are multiplied with the travelled distance of the vehicle and stored in the form of an emission event. As shown in Figure 1, emission events are stored in the general event log of a MATSim run, from which the simulated reality can be re-created after a simulation run has finished.

To validate their methodology, Hülsmann et al. (2011) conducted an experiment involving recorded vehicle trajectories, from which emissions were calculated using the detailed PHEM emission model with a temporal resolution of one second. The study finds significant variations in individual vehicular emissions

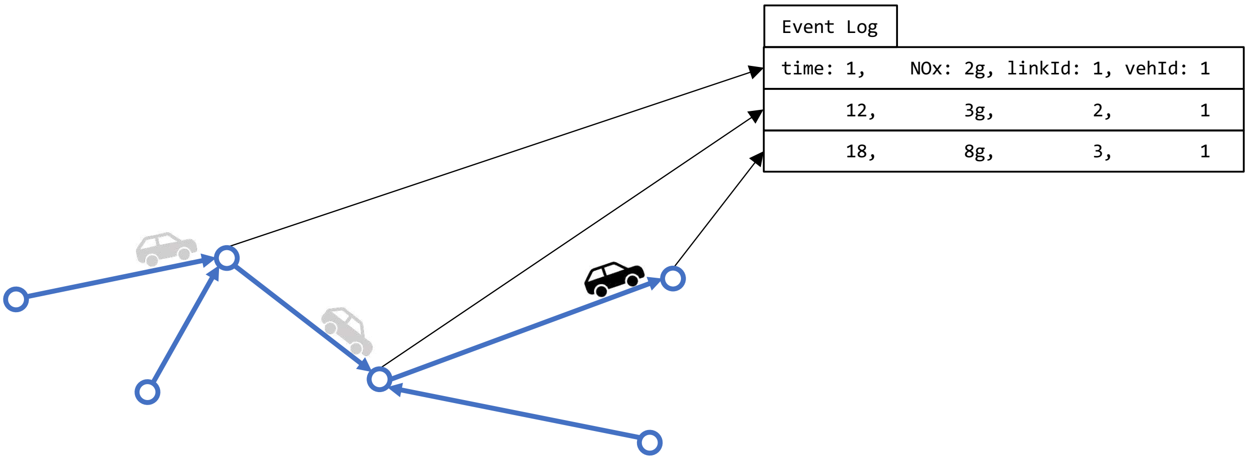

Figure 1: Example of emission calculation in the MATSim emission extension. A vehicle traverses three links on the simulation's street network, resulting in three emission events in the general event log. For simplicity, only NOx emissions are depicted. The emission extension is capable of calculating all the pollutants HBEFA provides emission factors for.

calculated with PHEM on the same link, even under similar traffic conditions. The averaged emissions calculated from the real-world vehicle trajectories were then compared to emissions calculated, using simulated traffic in MATSim and HBEFA emission factors, with the result that the presented emission tool is able to *"approximate emission levels that look similar to PHEM data and shows similar tendencies over time of day"* (Hülsmann et al., 2011, 13).

Conceptually, vehicular emissions based on HBEFA emission factors reflect the average emission that a typical vehicle with the same properties in the same traffic situation on the same type of link would have produced. This is comparable to using detailed vehicle trajectories with a high resolution, high-fidelity model such as PHEM and averaging the emissions afterward. The presented approach for calculating traffic emissions, retains the microscopic resolution of both the individual vehicles and the vehicle properties relevant for emission calculations, while employing an average value for the emission outputs. In consequence, when combined with a microscopic dispersion model, hot spots with exceeding levels of pollutant concentrations are the result of structurally unfavorable traffic conditions in combination with unfavorable meteorological conditions. An investigation of vehicular emissions with a temporal and spatial resolution finer than the size of a link is not feasible with the presented coupling approach. However, a spatial resolution on the link level is sufficient for investigating traffic emissions and their effects on a regional scale.

MATSim's emission module is currently also capable of estimating pollutant concentrations on a grid of receiver points (Agarwal, 2017) using a Gaussian Blur. However, the current method ignores important aspects of dispersion modelling such as wind, obstacles, chemical reactions or the height of the boundary layer.

2.3. Dispersion and air chemistry model

The urban climate simulation PALM-4U is a CFD model capable of operating in LES mode, simulating atmospheric boundary layer flows (Maronga et al., 2020). As it was designed to scale on massively parallel computing hardware, the model is capable of simulating large domains with fine grid resolutions (Maronga et al., 2019). In addition to resolving atmospheric turbulence, the PALM model system includes an atmospheric chemistry model (Khan et al., 2021) which is capable of simulating transport, chemical reactions and deposition of pollutants. The turbulence model in combination with the simulation of photochemical reactions allows for very detailed predictions of pollutant concentration in urban contexts as shown by Khan et al. (2021), making it possible to investigate pollution hotspots in a detailed manner.

3. Implementation of coupling method

The coupling of traffic emissions generated using MATSim, to the urban climate model PALM-4U is achieved seamlessly through the utilization of PALM-4U's chemistry module. The coupling of both models is carried out by converting MATSim output emission data into the PALM-4U chemistry driver file format (Maronga et al., 2020, p. 1353) The chemistry driver file format is part of the PIDS (PALM Input Data Standard) and is the preferred way of supplying emission information needed for the PALM-4U climate simulation. As MATSim and PALM-4U are programmed in different programming languages, implementing the coupling mechanism by exchanging data via input files allows running both models independently in different computing environments.

When converting MATSim output data into the chemistry driver file format, the problem of different spatial representations and differing temporal resolutions must be resolved. Spatial information in MATSim is modelled as vector data in Euclidean space, while the PALM model system divides the simulation domain into a regular raster where each grid cell covers a discrete volume. Results of a MATSim simulation are stored using a time step size of one second, while the PALM-4U chemistry module expects accumulated emission flows over uniform time periods. Additionally, traffic in MATSim is simulated on a network with simplified link geometries, to save computational resources, which interferes with high-resolution emission modelling. Hence, converting traffic emissions into chemistry driver input is conducted in four steps:

1. Mapping of detailed and simplified link geometries
2. Temporal aggregation of traffic emissions
3. Rasterizing of vector-based traffic emissions
4. Writing of the driver file

3.1. Mapping of detailed and simplified link geometries

Traffic in MATSim is modeled on a directed graph that consists of nodes (vertices) and links (edges). The links in the network represent streets and carry essential information for the mobility simulation, such as capacity, freespeed, and the number of lanes. Nodes, on the other hand, represent intersections where vehicles can switch from one link to another. Additionally, nodes contain geographical information about the network. MATSim networks are typically generated using OSM (OpenStreetMap) data, which is filtered for street-related information and then converted into the MATSim network format. During the conversion process, the original street network geometries are simplified, keeping only nodes with intersections in the MATSim network (see figure 2), thus reducing computational load and memory footprint during a MATSim run.

However, this abstraction is not suitable when it comes to modelling detailed traffic emissions. Simplified links might cut through occupied areas, as can be seen in figure 2, leading to traffic emissions being emitted from within buildings. To provide accurate emission flows to the chemistry model, the emissions calculated based on simplified link geometries must be mapped onto more detailed street geometries. Since the OSM data set originally used to generate the traffic network contains the required information, a mapping between the traffic network and the original geometries is established. During network generation from OSM data, the original street geometry is stored in the form of a link attribute containing a list of (ID, x, y)-triplets, which corresponds to the data model of a MATSim network node. With this information, a MATSim network with detailed link geometries can be re-created to calculate traffic emissions, while maintaining the advantages of simplified link geometries during the traffic simulation.

3.2. Temporal aggregation of traffic emissions

In the context of coupling MATSim and PALM-4U, it is important to be aware of differing time resolutions in the various steps of the modelling pipeline:

- MATSim functions at a high temporal resolution, processing data every second. This is evident as emissions in the MATSim event file are recorded with precise timestamps indicating the moment a vehicle exits a link.

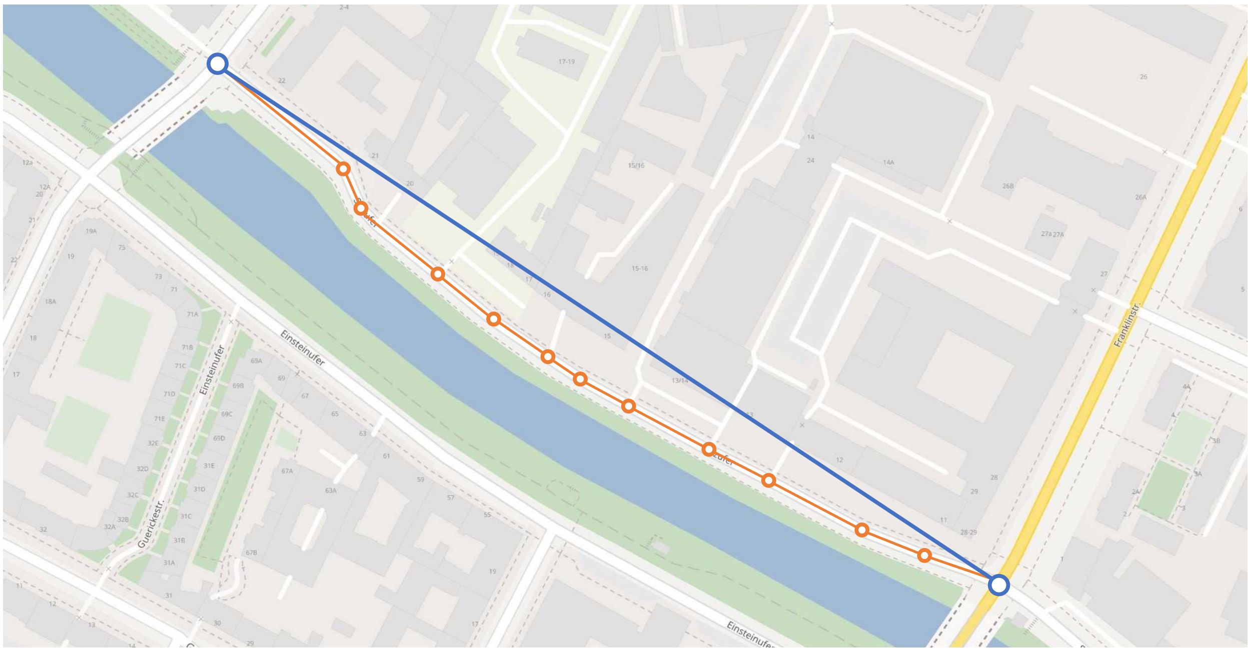

Figure 2: Example of a simplified street geometry in a MATSim network (blue) and its corresponding original geometry from OSM (orange)

- The time periods in the chemistry driver used in the idealized case study (see section 4) are set to one hour intervals. Though, due to recent advancements, the driver format now supports arbitrary time periods, at the time the idealized case study was conducted, only one hour periods were available. During each one-hour period, emission input into the PALM-4U simulation is constant.
- The internal transport equations in PALM-4U, as well as the calculations for pollutant concentrations and dispersion, are executed on the scale of seconds.
- The temporal frequency of the model's output, was set to hourly intervals for the purpose of our idealized case study.

As the temporal resolution of MATSim is one second, the produced traffic emissions must be aggregated into the time periods of the chemistry driver. Figure 3 illustrates this process with two time periods, each having a duration of one hour. All emission events with time stamps between 0, and, 3600 are sorted into the time period between midnight and 1am. All other events with time stamps between 3601 and 7200 are sorted into the time period between 1am and 2am. Within each time period, emission events are accumulated by link. For example, in the time period between midnight and 1am, link 2 is traversed by two vehicles each issuing 3g of NO_x (Nitrogen Oxides) accumulating to 6g of NO_x for link 2 during that time period. As the PALM model system uses a variable time step size in the magnitude of seconds, which is determined at runtime, the aggregated emissions from the chemistry driver are disaggregated during a PALM-4U simulation run. For each simulated time step within the same time period, the chemistry module releases a constant amount of emissions into the PALM-4U simulation domain. In the example of one hour periods, the amount of emissions released into the simulation domain for each time step changes once every hour.

As described in section 3.1, traffic emissions must be mapped onto detailed street geometries to achieve an accurate dispersion simulation, which is also done during the aggregation step of the conversion. According to section 3.1, a network with detailed street geometries is generated from the additional OSM nodes stored as link attributes. During the creation of the detailed network, a mapping is introduced which associates a simplified link with all the shorter links which were re-created from the detailed geometry information of

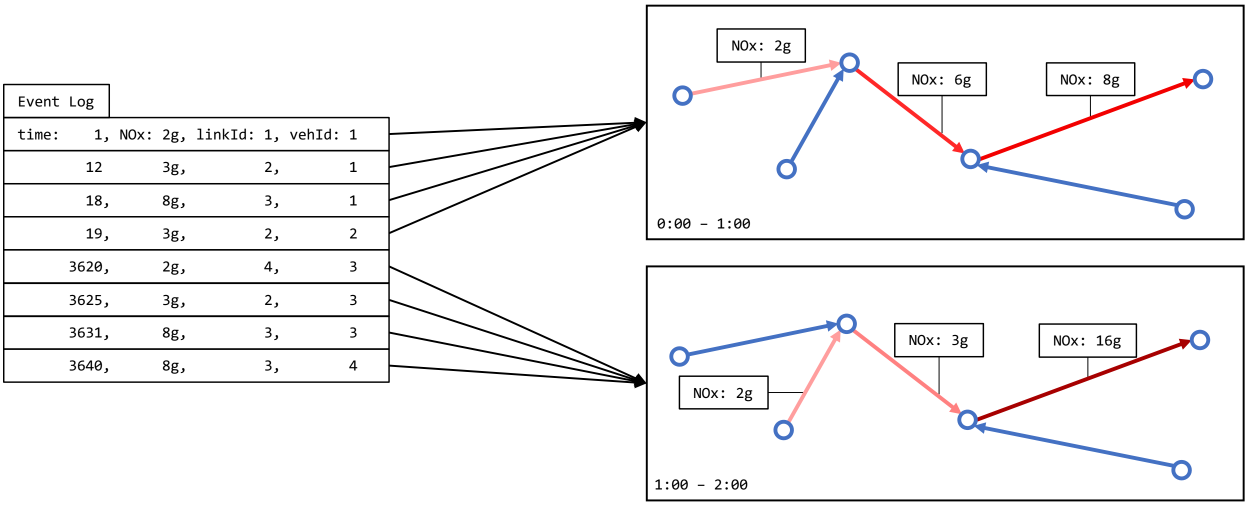

Figure 3: Aggregation step of emission events. Emission events from the event log are aggregated by time period. Within each time period, emissions of the same pollutant are aggregated by link.

that link. With the mapping between simplified and detailed links in place, aggregated traffic emissions for a simplified link can be distributed onto the detailed link geometries. The distribution of traffic emissions onto mapped links considers the length of each short link compared to the length of the simplified link.

Based on the HBEFA emission factors, MATSim generates separate values for particulate matter caused by the combustion process and particulate matter caused by other factors like breaks and tire abrasion. This is useful for studying certain policy cases, for example the electrification of the car fleet, where particulate matter caused by the combustion process would be eliminated, but the remaining particulate matter would still be present. The PALM-4U chemistry driver file is expected to contain the sum of emissions regardless of their source, separated by species. This requirement makes the aggregation of particulate matter stemming from the combustion process and other sources necessary and is performed during the aggregation phase of the pipeline.

3.3. Rasterizing of vector-based traffic emissions

The PALM model system is a grid-based model. Therefore, the link-based emissions from MATSim have to be converted into gridded emission data for the PALM-4U simulation. The traffic emissions, which were temporally aggregated in the previous step, must be distributed onto the raster chosen for the PALM-4U simulation. One raster with emission flows is required for each time period of the chemistry driver file. The process of distributing link-based emissions onto a raster is comparable to drawing lines on a screen, where vectors are translated onto a pixel grid. As it is fast and easy to implement, Bresenham's line drawing algorithm (Bresenham, 1965) is used as a basis to convert link based into raster-based emissions.

The implemented algorithm assumes that emissions for a certain link were emitted evenly across all cells covering that link. To determine the amount of emission per cell, the number of cells covering a link are counted in a first pass of the raster algorithm. In the second pass, the accumulated emissions for the current link are distributed evenly across all covering cells. This process is performed based on the detailed link geometries described in 3.1. Individual links vary in length from a few meters up to more than a hundred meters, depending on the geometry of the street they represent as well as the distance between intersections. In comparison, a resolution between one and ten meters is typically used to conduct PALM-4U LES mode simulations in urban set-ups. In the case of a raster cell covering more than one link, the emissions from all links are accumulated. Figure 4 shows how the emissions from the previous example are distributed onto the raster. For the links in red, emissions were calculated for the corresponding time period. The resulting emissions are distributed onto the raster, where darker shades represent higher emission flows. Furthermore,

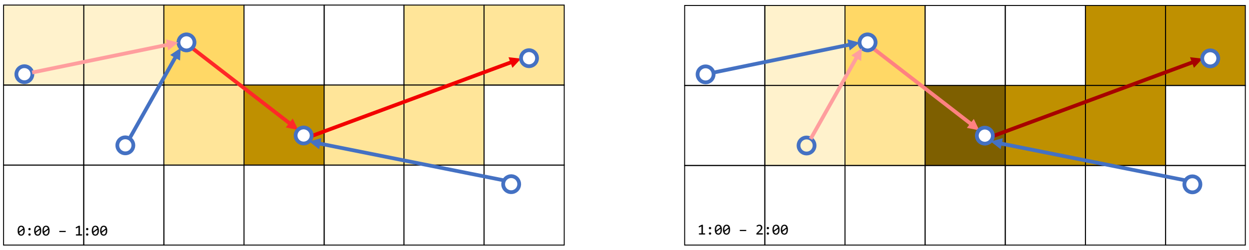

Figure 4: Rasterization step of aggregated emissions: A separate raster is produced for each time period of the simulation. Within each time period, the accumulated emissions of each link are distributed onto raster cells by the means of Bresenahm's line drawing algorithm.

it is visible that the raster cell with the highest emission flow covers multiple links. The described step is repeated for each time period and for each pollutant.

The MATSim emission model calculates values for NO_x and NO_2 (Nitrogen Dioxide) based on the corresponding emission factors in the HBEFA database. An accurate chemistry simulation, however, requires distinct values for NO_2 and NO (Nitrogen Monoxide). The missing NO values are calculated by subtracting NO_2 from NO_x after the raster step of the conversion. For each time period, the raster values of NO_2 are subtracted from the NO_x raster values.

3.4. Chemistry driver file

The transformed emission data is written into a chemistry driver file, which contains the emission information necessary to run a PALM-4U simulation. The driver file format (Maronga et al., 2020, 1353) is part of the PIDS (PIDS_Chem) and contains rastered emission information divided into uniform time periods. The file structure is based on the NetCDF standard, which was designed to accommodate multidimensional raster data. The information about time periods, species and the x, y coordinates are stored in separate indices in the file, which allows for random access by those dimensions. Based on the transformations described in the previous sections, the chemistry driver file is populated with traffic emissions for each raster cell and each time period separated by species.

Figure 6a shows the content of a chemistry driver file for the PALM-4U model setup used in section 4. The image shows NO_2 emission flows into the PALM-4U model setup for the time period between 8am and 9am for a 6.7Œ6.7ăkm model domain with a 10m grid resolution. NO_x has already been split up into NO and NO_2 by subtracting NO_2 from NO_x as described in section 3.3. The overall pattern of emission flows corresponds to the hierarchy of the street network. Major roads, as well as the inner-city freeway, produce high traffic emission flows, while minor streets appear less pronounced. The driver file in figure 6a additionally contains emission values for particulate matter, NO and O_3 (Ozone).

The PALM model system requires simulations to run in UTC time format. Since attributes such as sun radiation play an important role, it is crucial to know what time ad date it is. MATSim, on the other hand, is date-agnostic and only counts seconds from the beginning of the simulation. Usually, a MATSim simulation begins at midnight local time, so that a conversion of MATSim time stamps into UTC time is necessary. This step is performed during the writing phase of the processing pipeline.

4. Application of coupling method

The capabilities of the developed coupling mechanism are demonstrated by conducting an idealized case study in Berlin, the capital of Germany. The focus of the presented study lies on investigating the relationship between traffic dynamics and pollutant concentrations. A key aspect of our investigation involves a critical evaluation of the coupling approach itself under idealized conditions. To achieve this, we deliberately idealized our input parameters, simulating traffic patterns representative of a typical day and imposing a constant and notably slow wind speed of 1 m/s. This deliberate choice of a low wind speed stems from our hypothesis that such conditions could lead to elevated pollutant concentrations, reflecting the impact of

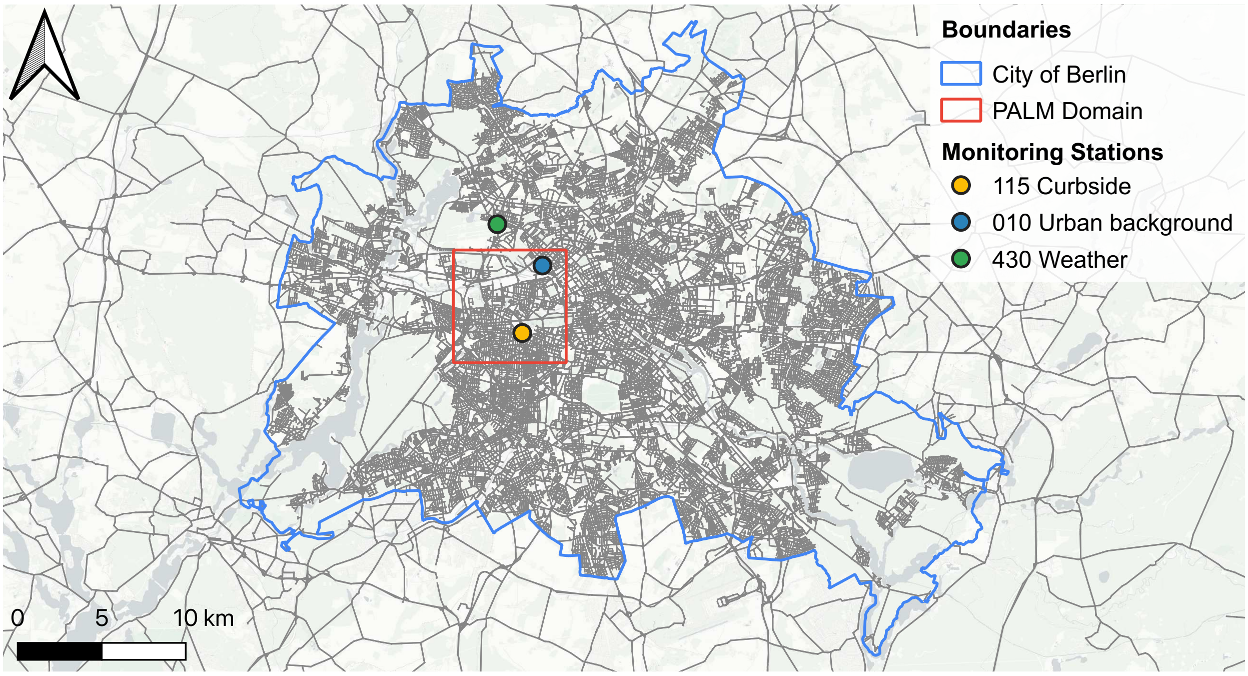

Figure 5: The city boundaries of Berlin (blue), as well as the PALM-4U-Domain boundaries (red). Within the city boundaries, a detailed road network (gray) is included. For the remaining MATSim domain, only major roads are included. The MATSim traffic simulation setup stretches beyond the depicted area.

diminished atmospheric dispersion. Importantly, our study also seeks to demonstrate the capability of our approach to identify emission *hot spots* in a large urban environment simulation, using pre-existing MATSim and PALM-4U setups.

4.1. Existing MATSim and PALM-4U setups used for the application

The Open Berlin Scenario (Ziemke et al., 2019; vsp-gleich et al., 2023) setup serves as the basis for calculating traffic emissions. It encompasses the city of Berlin (blue border in figure 5), as well as a part of the surrounding state of Brandenburg. The traffic simulation setup includes 494,107 simulated persons, which corresponds to a 10% sample of the population of Berlin and Brandenburg. To compensate for the sampled demand, Ziemke et al. (2019, 875) reduce the flow and storage capacities of the road network accordingly, to achieve comparable traffic dynamics as if the entire population were represented in the simulation setup. Therefore, a single vehicle travelling on the simulated network represents ten vehicles in reality and emissions produced by a simulated vehicle must be multiplied by a factor of 10 to compensate for the sampling of the traffic demand. A detailed road network, generated from OSM data, including all road types from motorway to the residential level, is available within the city boundaries of Berlin, as shown in figure 5. For the surrounding federal state of Brandenburg, a street network including major and secondary roads is used. The traffic simulation setup also includes a timetable-based public transportation system generated from a GTFS (General Transit Feed Specification) dataset available for Berlin and Brandenburg. The simulated persons included in the traffic simulation setup can adjust their behavior by either switching modes of transport, selecting different routes within the same mode, or adjusting the departure times of their trips.

As preparation for the presented study, a new network is generated from OSM data to provide detailed road geometries necessary for creating the chemistry driver file as described in section 3.4. Since the traffic simulation is conducted on a new road network which includes data to reconstruct detailed road geometries (see section 3.1), all route information referencing the old network must be cleared from existing plans held by simulated persons. To let the traffic simulation adapt to the new network, 100 iterations are performed until a new equilibrium as described in section 2.1 is reached. To accelerate the process, simulated persons are only allowed to adapt their behavior by adjusting routes, instead of also selecting different modes of transportation or adjusting departure times of their trips. Based on the newly created traffic simulation setup, traffic emissions are calculated and subsequently, using the conversion method presented in section 3, the chemistry driver file is created for the domain covered by the PALM-4U setup (figure 5 red area). The temporal resolution of the emission flows in the chemistry driver are set to one hour, as this was the only available temporal resolution option at the time the study was conducted. Figure 6a shows the result of the NO_2 emission calculations and the subsequent conversion for the period between 8 and 9 am.

For the dispersion calculation, the Berlin model created by Khan et al. (2021); Khan (2020) is used and supplemented. The covered model area is shown in red in Figure 5. It includes a square area with a side length of 6.71 km and extends 3.6 km vertically. The grid used has a resolution of 10 m in the horizontal and vertical direction. Above the height of 2.7 km, the resolution gradually becomes coarser in vertical direction. The model also includes road types, building heights, water bodies, soil conditions, and vegetation. The simulation is configured for July 17, 2017, chosen as a "typical Berlin" summer day with temperatures between 16 and 25 °C, scattered clouds, and predominantly westerly winds. For traffic emissions, the original setup uses the parameterized LOD (Level of Detail)0 emission mode, where traffic emissions are based on road types and a simplified diurnal profile.

The PALM-4U chemistry module accepts input emissions with varying LOD, where LOD0 is the default, providing parameterized emissions following a diurnal profile for major and minor road categories. The original PALM-4U setup is adjusted to run in LOD2 mode, in which input emissions for the PALM-4U simulation are provided by a chemistry driver file. Instead of using parameterized traffic emissions, the adjusted PALM-4U model setup uses emissions generated with the MATSim traffic model, which were transformed into the PALM-4U chemistry driver format using the methodology described in section 3. Four species: NO, NO_2, PM_{10} (Particulate Matter), and O_3, are simulated, using the photo stationary state mechanism (PHSTAT) for the gas-phase chemistry. Additionally, dynamic wind speeds and wind directions are deliberately simplified to a steady wind flow of 1m/s from a western direction. This simplification replaces the realistic variations in wind conditions throughout the day with constant values, providing a controlled environment to explore the specific effects of traffic emissions on dispersion patterns. To provide sufficient spin-up time, two consecutive days are simulated using the same 24h traffic emissions. The following analysis is conducted using only data from the second day, which corresponds to the 17th of July 2017, as in the original model set up.

4.2. Simulation results and discussion

For the conducted PALM-4U simulation, averaged masked output files are produced. The averaging interval is set to one hour, matching the temporal resolution of the input traffic emissions. The mask follows the terrain structure, giving all raster cells with the same z-index the same height above ground. The following investigations are conducted on the bottom layer of the averaged masked output, which covers the layer that extends from the ground up to a height of 10 meters. Figure 6b shows averaged NO_2 output concentrations of the conducted PALM-4U run for the time between 8 and 9 am. The overall pattern of pollutant concentrations represents the pattern of input emissions from the chemistry driver file in figure 6a. Street segments with high traffic volumes and high emission flows seem to produce higher pollutant concentrations within their vicinity. This way, major roads like the inner-city freeway on the left, and arterial roads are clearly recognizable.

To assess the plausibility of the simulated air pollution concentrations, a comparison is conducted between simulated and observed NO_x concentrations. The simulation domain of the PALM-4U setup encompasses two monitoring stations: one curbside and one urban-background station (Senatsverwaltung für Mobilität, Verkehr, Klimaschutz und Umwelt). The comparison focuses on the urban-background monitoring station 010, located in the northern part of the PALM-4U simulation domain. Curbside station 115 is influenced significantly by frequent diesel bus traffic due to its proximity to a major city bus hub and is excluded from this comparison (Schümann et al., 2021).

Figure 7 presents a comparison of simulated NO_x concentrations with monitoring data at the urban-background station 010. In the plot, hourly average concentration values from the simulation, at the raster

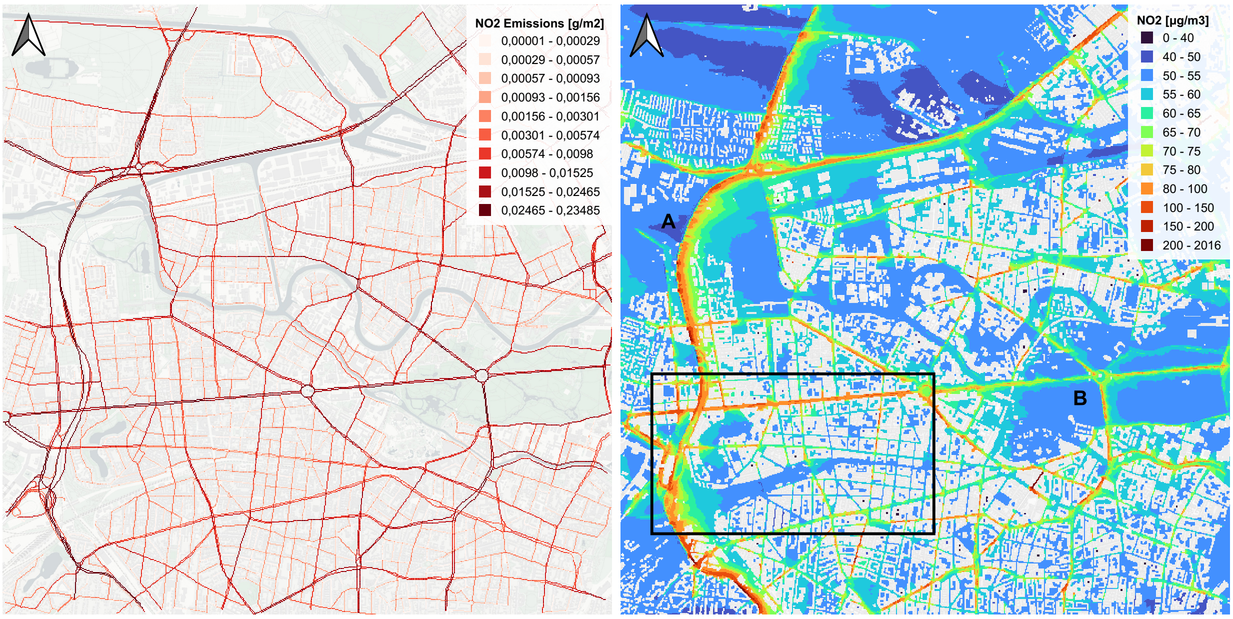

(a) (b)

Figure 6: (a) Rastered emission flows in g/m^2 for the period between 8am and 9am; Emission flows in (a) are the output of the MATSim emission model and the raster pipeline, NO_x has already been split into NO and NO_2. Figure (b) shows the corresponding NO_2 concentrations simulated with PALM-4U for the same time period. The area of the rectangle in (b) corresponds to figure 8

point closest to the monitoring station, are depicted in red. The hourly concentration values from the monitoring station are shown in varying shades of blue. The simulation setup represents an artificial day, incorporating traffic volumes typical for a workday and constant low wind conditions of 1 m/s from the western direction. To ensure a suitable basis for comparison, we select measured data from June, July, and August, specifically choosing the five days with the lowest average wind speeds. Average wind speeds measured at weather monitoring station 430 Tegel (DWD-Deutscher Wetter Dienst) during these selected days range from 1.3 m/s to 1.7 m/s, with lower speeds (between 0 m/s and 2 m/s) in the morning hours (midnight to 8 am) and higher speeds (between 1 m/s and 3 m/s) from 8 am to 6 pm. Wind speeds during the remaining evening hours are similar to those in the morning.

Examining Figure 7, simulated NO_x concentration levels hover around 50 $\mu g/m^3$ from midnight to 4 am, followed by an increase between 4 am and 9 am, peaking at 103 $\mu g/m^3$ at 6 am. From 9 am to 8 pm, NO_x concentrations decrease from 47 $\mu g/m^3$ to 23 $\mu g/m^3$ before rising again during the subsequent simulated hours. Analysis of the monitoring data reveals a varied picture during the early night hours (1 am to 4 am), with three days exhibiting relatively low concentration values (13 $\mu g/m^3$ to 40 $\mu g/m^3$) and two days showing notably higher values (up to 105$\mu g/m^3$). On all selected days, a concentration peak is observed in the morning hours between 8 am and 9 am, except for one day with a peak at 7 am. Between 9 am and 8 pm, NO_x concentrations decline on all selected days before increasing again during the later hours.

Comparing simulated, and measured concentration levels reveals a similar daily pattern. Early night and morning hours exhibit relatively low concentration values, followed by a morning peak. Concentrations during the remaining daylight hours remain relatively low before rising during late-night hours. Simulated NO_x concentrations align within the range of measured values for respective hours of the day, except for the period between noon and 4 pm. During these hours, wind speeds at weather monitoring station 430 were higher than 1m/s on all selected days, which might have led to a higher rate of dispersion compared to the simulation. Notably, the peak in concentration values for the simulated data occurs earlier than for the measured data. This observation suggests a limited presence of turbulence in the model during the early morning hours when the boundary layer remains stable, contrasting with real-world conditions. In

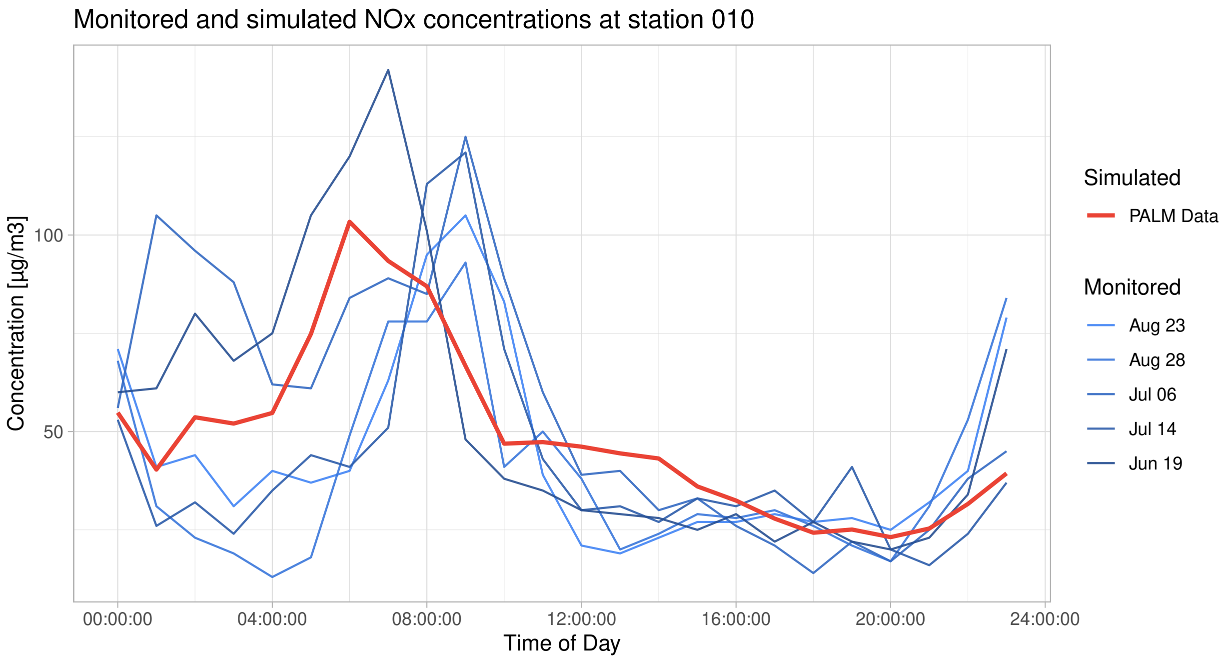

Figure 7: Comparison of simulated and monitored NO_x concentrations at urban background monitoring station 010. Simulated hourly averages of NO_x concentration values are depicted in red; Hourly averages of monitored NO_x concentration values at urban background station 010 for days with low wind speeds in blue tones.

the model, turbulence is primarily generated by wind and radiation, while in reality, additional factors such as turbulence induced by moving vehicles may contribute to a greater dispersion of pollutants, surpassing what can be observed in the current model setup.

Though the overall pattern of pollutant concentrations in figure 6b is dominated by traffic volumes, investigating concentration levels in more detail reveals other factors which have a high influence on concentration levels:

- Wind Direction
- Building and Street Layout
- Time of day
- Raster and simulation artifacts

The subsequent sections give a comprehensive examination of these factors. The simulation carried out generated concentration data for NO, NO_2, PM_{10}, and O_3, among which NO_x and PM_{10} are pertinent pollutants in relation to health impacts. To maintain brevity in the discussion of results, the subsequent analysis primarily centers on NO_2, as the observed effects align with those noted for PM_{10}.

4.2.1. Wind direction

Wind direction has a major influence on concentration levels observed in the PALM-4U output data. In the area surrounding point A in figure 6b, high pollutant concentrations are noticeable along the inner-city motorway. Since the motorway is not obstructed by buildings, the traffic emissions are transported with the wind direction and gradually dissipate. A similar effect can be observed for the area around B where emitted pollutants dissipate evenly to both sides of streets which are parallel to the general wind direction and dissipate with the wind for streets perpendicular to this direction. Notably, obstructed roads exhibit distinct dispersion patterns, as detailed in section 4.2.2.

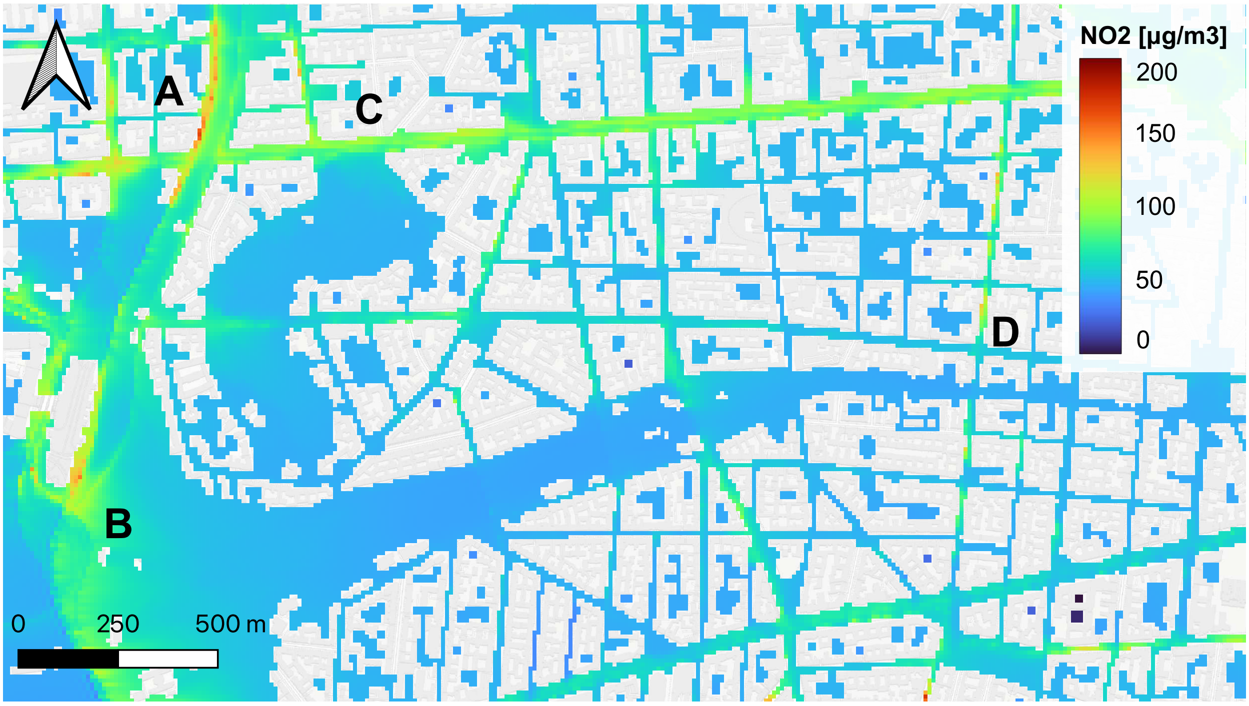

Figure 8: NO_2 concentrations on a continuous scale. The area depicted corresponds to the rectangle in figure 6b. Effects of the building layout as well as the street layout are highlighted by letters A - D

4.2.2. Building and street layout

The layout of buildings surrounding street corridors influences the simulated pollutant concentration levels. The areas around A, B and C in figure 8 represent distinct layout situations and their influence on pollutant concentration levels. The color ramp in figure 8 is capped at $200 \mu g/m^3$, effectively excluding 0.04% of outliers (see section 4.2.4) in the 8 am time period, and reveals concentration patterns on a smaller scale.

The effects of the building layout interact with the general wind direction as can be seen when investigating concentrations close to the city motorway near A and B in figure 8. Both motorway sections have comparable traffic volumes, but show different concentration levels. The motorway section around B has almost no buildings in the vicinity which lets air flow over the motorway without obstructions. Traffic emissions are taken up from the street level and transported with the wind direction while being diluted in the process. In contrast the motorway section near A is situated in a different topology. Both sides of the motorway are obstructed by relatively high buildings forming a wide street canyon. Within that street canyon pollutant concentrations are generally higher compared to the area around B. As the motorway section is situated in a street canyon topology, traffic emissions cannot be transported freely with the wind direction but are retained within the street canyon. Within the street canyon traffic emissions are especially high close to buildings situated on the upwind side of the motorway. This effect is caused by eddies forming behind obstacles that obstruct the wind flow. While the air flow at the roof level follows the general wind direction, the eddy caused by the obstructing building reverses the wind direction at street level. The traffic emissions emitted by vehicles travelling on the motorway are therefore transported towards the buildings on the western side of the motorway leading to high pollutant concentrations.

Another effect of building layout can be observed in area C in figure 8 where we have comparable pollutant concentrations to area A. Due to the building layout along the street, a narrow street canyon is formed from which traffic emissions cannot dissipate leading to high concentration levels even though traffic volumes on the arterial road are roughly half of what can be observed on the city motorway.

In addition to the building layout, pollutant concentrations are influenced by the street layout relative to the overall wind direction. The area around D in figure 8 shows NO_2 concentrations for the intersection of KantstraSSe/LeibnitzstraSSe, of which both streets have comparable traffic volumes. Still, the street perpendicular to the overall wind direction causes higher pollutant concentrations due to the street canyon effect (described above) which captures traffic induced pollutants within said street canyon. For the street parallel to the overall wind direction emissions are transported along the street corridor and eventually dissipate.

Additionally, elevated pollutant concentrations are observed in shaded areas, contrasting with lower concentrations in sun-exposed regions. This distinction arises from the temperature variation between shaded and sunlit areas, where the latter experience higher temperatures due to direct sun radiation. The temperature discrepancy influences the vertical motion of air, with colder areas exhibiting reduced upward transport compared to warmer regions. This diminished vertical transport results in higher pollutant concentrations in colder, shaded areas. Notably, for NO_2, an additional factor comes into play where, in the absence of sunlight, the photochemical reaction essential for breaking down NO_2 into NO and O_3 does not occur. Consequently, NO_2 persists in the atmosphere, contributing to higher NO_2 concentrations in shaded areas. Both effects are also described in the analysis of the original PALM-4U setup provided by Khan et al. (2021).

4.2.3. Time of day

Figure 7 shows simulated NO_x concentration levels in comparison to measurements of urban background monitoring station 010. Examining the output concentration levels of the PALM-4U setup depicted in red, reveals a high fluctuation during different hours of the day with a peak for NO_x concentrations beetween 6 and 8am. During that time period of the day, the morning traffic rush hour has already started, while the atmospheric boundary layer is still relatively shallow and upward transport by convection has not yet fully started. The remainder of the day shows much lower NO_x concentrations on the ground levels as upward transport as well as photo chemical reactions reduce concentration levels in the bottom layer of the atmospheric model. This process is also described in the model analysis presented by Khan et al. (2021).

The temporal variation in pollutant concentration appears significantly more pronounced than the spatial variation within a given time period. Examining simulated concentration levels from figure 7 reveals a notable fluctuation in NO_x concentrations, with a factor of 4.5 difference ranging from $23.1\mu g/m^3$ at 8 pm to $103.3\mu g/m^3$ at 6 am. In comparison, the simulated NO_x concentrations for all grid points between 7 and 8 am show a much narrower range, varying only between $81.4\mu g/m^3$ and $95.0\mu g/m^3$ for the 50% values closest to the median value over the model domain (excluding outliers exceeding $200\mu g/m^3$). This observation suggests that the primary influence on concentration levels is the time of day, attributed to the upward transport of pollutants and the occurrence of photochemical reactions.

4.2.4. Artifacts

The distribution of concentration levels shows a very long tail of higher than average concentration levels for the individual time periods. The majority of simulated concentration values lie within a small range below $100\mu g/m^3$, as described in section 4.2.3, while maximum concentration levels reach up to $2000\mu g/m^3$. Investigating raster cells with concentration levels higher than $200\mu g/m^3$ (representing 0.016% of all values) reveals different patterns of outliers, sorted from most to less severe:

1. **Raster Artifacts:** The highest concentration levels can be observed due to artifacts as a result of the rastering process. The leftmost map in figure 9 gives an example of such a case. The underlying street has a relatively high traffic volume, while the rastering algorithm to generate the static driver of the PALM-4U model decided that tiles covered by the street are in the simulation covered by buildings. The emissions produced with MATSim are then distributed onto the remaining raster tiles covering that link. This leads to very high concentrations in the first place because emissions that were emitted over the entire length of the link are mapped onto a smaller number of raster cells, then what the length of the link would suggest. In this particular case, the wind direction blows emissions into the artificial dead end at the end of the street corridor, leading to even higher simulated concentrations.

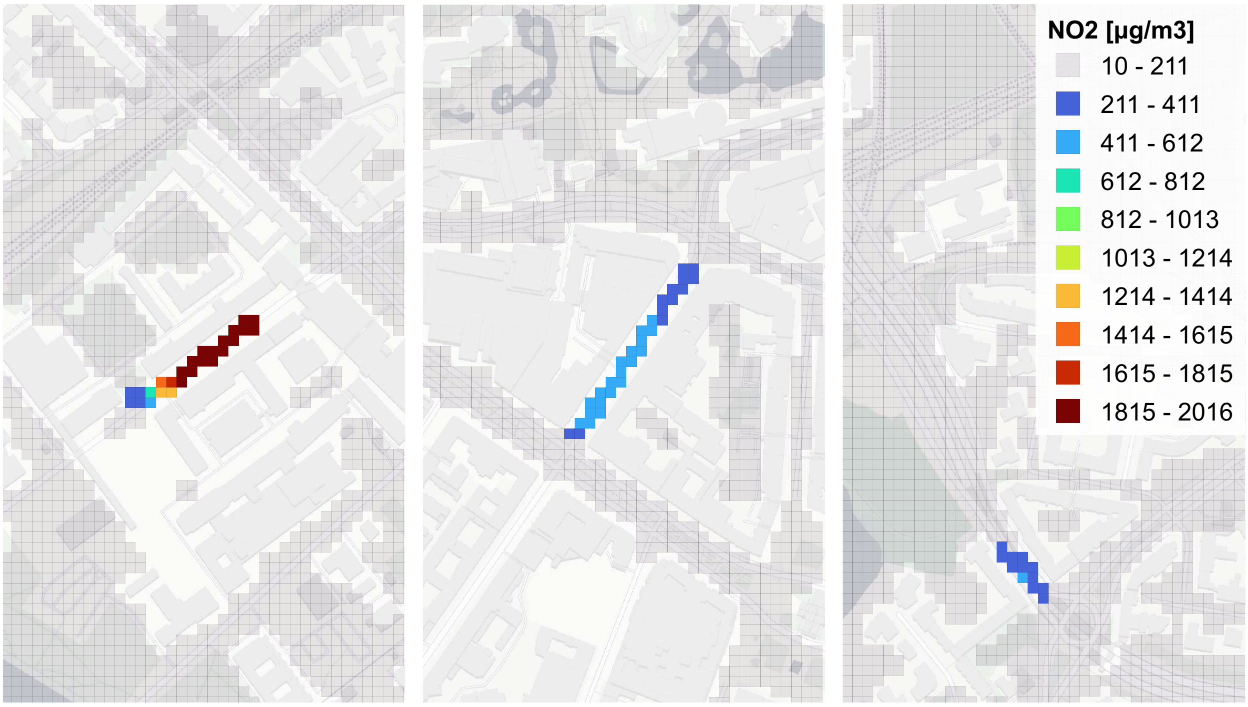

Figure 9: NO_2 concentrations for the time period between 8am and 9am, showing areas with exceptionally high pollutant concentrations due to artifacts in the simulation set up. The coloring uses equal intervals to highlight outliers on the long tale of the concentration value distribution.

2. **Resolution and Grid Layout:** Due to the relatively coarse resolution of 10m, streets lying in narrow street canyons are sometimes represented by only a single pixel row. The map in the center of figure 9 demonstrates this issue, where a street with moderate traffic volumes causes high pollutant concentrations. The angle at which the street canyon is situated compared to the grid structure forms multiple caverns where turbulence does not correctly form and pollutants are not transported away from the ground level.
3. **Stacked Streets:** The rightmost map in figure 9 shows another special case where exceedingly high pollutant concentrations can be observed. In the case depicted, the model has two stacked street levels. The lower one is a six lane motorway, while the upper one is a four lane arterial road. As the implemented mechanism does not resolve emission flows in vertical direction but assumes all emissions to emerge from ground level, the emissions of both streets are emitted into the same raster tile, leading to high pollutant concentrations.
4. **Numerical effects:** The applied raster method distributes emissions from one link onto a single line of raster cells. This leads to numerical effects in the CFD model causing less pronounced dispersion of traffic emissions for links situated in areas without obstructions.

Mitigating the listed types of artifacts could be accomplished with different strategies. The most straightforward improvement would be to increase the resolution of the simulated setup, which would solve item (2) at the cost of higher computational demands. For the mitigation of numerical effects (4) the raster algorithm must be switched to an algorithm which accounts for the width of the simulated street, distributing the rastered emissions on a line which is wider than a single pixel. This improvement would also require a higher resolution of the model grid to achieve a substantial improvement. Avoiding concentration outliers due to raster artifacts (1) could be accomplished by applying a pre-processing before the PALM-4U simulation starts. Raster cells that are labelled as buildings but for which the chemistry driver provides traffic emissions, could be re-labelled as streets in the static driver file. Adjusting the static driver in that way, would ensure that streets are not covered by raster cells labelled as buildings, so that emissions produced on a link can be distributed over the entire length of the link, avoiding exceedingly high emission flows in the chemistry driver. Modelling stacked streets (3; correctly is not trivial and would require changes on both models. The traffic model would have to have information on the vertical layout of streets, while the chemistry driver would have to provide the ability to place traffic emission sources in vertical direction. Modelling stacked structures like bridges correctly would also require a higher resolution of the simulation setup, at the expense of increased computational costs.

4.2.5. Detecting pollutant concentration emission hot spots

The simulation results of the coupled traffic emission and dispersion models allow the detection of traffic induced pollution hot spots. These are the areas which are significantly impacted by traffic emissions. Pollution hot spots can be defined in multiple ways, the most common one being ambient threshold concentration values which must not be exceeded within a certain time period.

EU-regulations define a annual mean limit value of $40\mu g/m^3$ for NO_2, as well as an hourly limit value of $200\mu g/m^3$, which must not be exceeded by more than 18 hours per year (European Environment Agency, 2020). The monitoring of these threshold values is conducted with curbside monitoring stations. For the simulated domain, two air quality monitoring stations are situated in the simulation domain as shown in 10a. Compared to the point-based monitoring, the introduced mechanism allows for a comprehensive investigation of threshold violations within the simulated domain. Figure 10a shows threshold violations for an arbitrary threshold of $80\mu g/m^3$ which was selected to receive a spatially differentiated image for the time period between 8 and 9am. The image shows that large parts of the motorway, as well as most of the major roads, cause concentrations above the chosen threshold value, especially when situated within a street canyon perpendicular to the wind direction. Figure 10a also shows that both monitoring stations are not affected by the threshold violations, indicating that, their position does not correspond to where the highest pollutant concentrations are to be expected, at least for the simulated west wind weather conditions.

As health effects due to pollution do not correspond to threshold values, another possible way of mitigating health effects is to limit a population's exposure to such pollutants. The Open Berlin Scenario setup, used for our idealized case study, incorporates calibrated activity locations and times, as described by Ziemke et al. (2019). With access to activity locations and times in MATSim it is straightforward to calculate an exposure index for raster tiles of a simulated PALM-4U domain. Activities which are situated within raster tiles marked as buildings are mapped onto the closest outside raster tile. The observed concentration value c_p is then multiplied with the time t_a spent within this raster tile at the given concentration, as shown in equation 1:

$$E = t_a * c_p \tag{1}$$

Applying this method to the simulation domain yields Figure 10b, which indicates that exposure hot spots are not necessarily situated where the highest pollutant concentrations can be observed. The northwest part of the inner-city motorway, where high pollutant concentrations can be observed, does not pose a large problem, when evaluating traffic emissions by exposure impact, as this stretch of the motorway is situated in an area with low activity density. In comparison, other areas with lower absolute pollutant concentrations cause much higher exposure to traffic emissions due to higher density of activities. The proposed exposure investigation is limited to time spent at activities and ignores exposure to pollution experienced during trips.

4.3. Comparison to other studies

Two studies referenced in section 1 have conducted similar studies to what we have presented, computing detailed emissions from traffic simulations and calculating pollutant concentrations using CFD models.

San José et al. (2021) use SUMO (Simulation of Urban MObility) (Alvarez Lopez et al., 2018) as their traffic model, the EMEP/EEA Air Pollution Emission Inventory Guidebook (EMEP/EEA, 2016) to generate emissions from traffic, and MICROSYS (José et al., 2008) as meteorological model. SUMO, similar to MATSim, follows individual vehicles, but other than MATSim computes values for acceleration and braking. However, the EMEP/EEA approach uses HBEFA, i.e. the same data that we use, as their sub-model for traffic, and in consequence the end result is quite similar to ours in the sense that acceleration and braking are

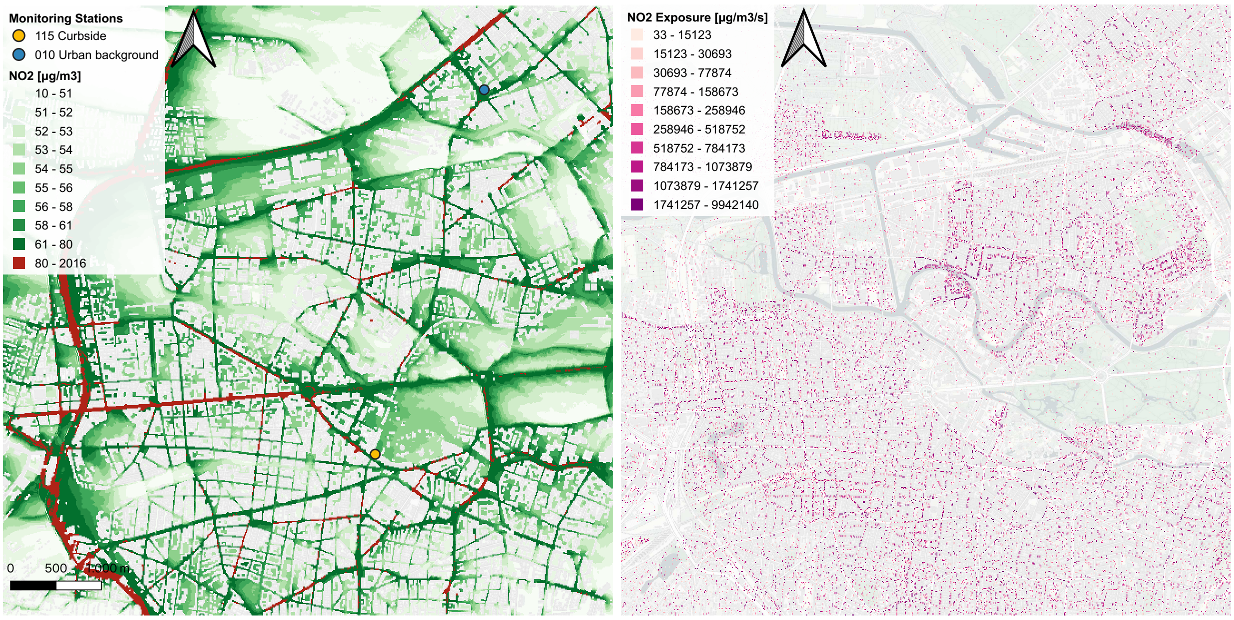

(a) (b)

Figure 10: Two methods to identify emission hot spots: Figure (a) uses a threshold approach showing NO_2 concentrations below and above $80\mu g/m^3$, and two curbside monitoring stations. Figure (b) shows exposure to traffic emissions at activity locations.

ignored and instead average emissions values are looked up based on traffic and road conditions. MICROSYS is a CFD-RANS model and thus steady state, in contrast to the PALM model system which we operate in LES mode. Traffic demand in San José et al. (2021) is generated from counting stations, which is possible because the study considers a relatively small area. Thus, our study is quite similar to theirs, with the following important differences:

- In our work, the traffic demand is driven by a regional behavioral model. This allows, in future studies, to investigate behavioral responses to possible traffic demand management measures, which might be considered in order to improve air quality.
- The area covered by the domain used for the PALM-4U simulation is much larger than what was used in the study conducted by San José et al. (2021). Covering larger parts of the city is important to derive traffic management policies and their evaluation.
- In our work, a fully dynamic meteorological model is used, which we consider a more appropriate approach to the complex topologies of urban situations.

The study conducted by San Jose et al. underscores the importance of high-resolution modelling for a more accurate understanding of pollutant concentrations in urban areas with complex topography. In contrast to our findings, they find elevated pollution concentrations on the downwind side of street canyons. Conversely, our results indicate that high pollution concentrations are to be expected at the upwind side of street canyons as described in section 4.2.2. Their divergent results can be attributed to the different computational approaches employed in both studies. San Jose et al. utilize the RANS method, which, because of its eddy parametrization, might not as effectively capture the turbulence dynamics within street canyons. On the other hand, our study employs the PALM model system in LES mode, which accurately simulates the predominant turbulence patterns in street canyons.

The second study, conducted Sanchez et al. (2017), uses VISSIM as their traffic model, and TNO ENVIVER based on VERSIT+ micro (Smit et al., 2007) to generate emissions from traffic. Their meteorological model appears to be a unique RANS model. VISSIM, similar to SUMO, follows individual vehicles with acceleration and braking. The VERSIT+ micro approach, while bearing similarities to HBEFA in its use of lookup tables based on traffic and road conditions, is a distinct development by the Netherlands Organization for Applied Scientific Research independent of HBEFA. The publication does not specify the generation of the traffic demand and focuses on the investigation of one complex intersection. In consequence, the study presented by Sanchez et al. operates on a smaller (more detailed) scale. Other differences to our approach are similar to those given for San José et al. (2021) in the paragraphs above.

5. Conclusion and outlook

The paper describes a methodology to couple the turbulence and building resolving PALM model system with the traffic and emission model MATSim. The implemented coupling mechanism is realized, converting MATSim output data into the input format required by the PALM-4U chemistry driver. This conversion involves translating between the fundamentally different data layouts of both simulation models. In particular, vector and event-based emission data must be converted into the grid and time period-based data layout required to execute the PALM-4U chemistry model with pre-processed emissions (Maronga et al., 2020, p. 1353).

The proposed coupling mechanism enables microscopic emission and dispersion modelling on a larger scale than what was possible so far. In contrast to the literature reviewed in section 1, MATSim is capable of simulating traffic on the scale of entire regions, including several hundred thousand vehicles on the simulated street network. With HBEFA emission factors, emissions are calculated based on: individual vehicle properties, the current traffic situation and characteristics of the street a particular vehicle is travelling on. Due to its scalability onto large high-performance computing clusters, PALM model system, on the other hand, is capable of simulating the atmospheric boundary layer of entire city districts while maintaining a fine grid resolution, enabling the prediction of very accurate pollutant concentrations induced by traffic pollution. The CFD approach for modelling emission dispersion in combination with the simulation of atmospheric chemistry reactions provides more fine-grained results compared to operational or other parameterized dispersion models.

Combining high-resolution traffic emissions with fine-grained pollutant dispersion modelling enables better identification of pollutant concentration hot spots. Currently, curbside monitoring stations are used to quantify air pollution levels in cities, but this approach is limited in its ability to capture a comprehensive view of pollution levels due to the limited number of monitoring sites. For instance, Germany's capital Berlin has only 16 air quality monitoring stations at the time of this writing. The proposed coupling can be employed to comprehensively model air pollution levels within entire city districts and to identify concentration hot spots caused by traffic air pollution.

Furthermore, the presented coupling mechanism, facilitates the possibility to implement and evaluate mitigation strategies for pollutant concentration hot spots. Based on identified areas with problematic concentration levels, traffic management schemes can be designed and implemented in the traffic model. With the changed traffic patterns resulting from the implemented management schemes, traffic emissions are generated and used as an input for another PALM-4U simulation with which it is possible to evaluate the effectiveness of the applied policies. The procedure can be iterated until the desired effects on pollutant concentrations are achieved. This process enables the rapid prototyping of traffic emission mitigation strategies, offering policymakers a valuable design tool, and will be presented in a follow-up study.

The study presented in section 4 uses simulated traffic that represents a typical workday in Berlin. In alignment with that assumption, the meteorological setup models a typical summer day, with artificial low wind conditions, applying a constant wind direction and speed. Though sufficient for demonstrating the technical capabilities of the presented coupling mechanism, a full validation run with realistic meteorological conditions is necessary. To achieve realistic results, it is probably necessary, to also enhance the simulated traffic to represent the specific date simulated with the PALM-4U setup. Validation runs representing specific dates and their weather conditions are part of the UC^2 project and currently conducted by the University of Hannover, Germany.

The presented coupling mechanism allows new applications for studying traffic induced emissions as well as the application of traffic management schemes. Still, the proposed method requires the aggregation of emission data calculated for individual vehicles in the spatial and temporal dimension. With MATSim it is possible to render vehicle positions for each time step of the simulation. The included emission module could be extended to calculate emissions based on these positions, greatly improving the granularity of generated traffic emissions, compared to the current state, where emissions are generated per link. The ongoing development of a study involving high-resolution coupling of vehicle emissions on a per-time-step basis holds the potential to facilitate the tracking of emission dispersion for individual vehicles within PALM-4U. Additionally, it enables the modelling of turbulence generated by vehicular traffic, a factor that significantly impacts the dispersion of traffic emissions within street canyons, as demonstrated by previous research (Zheng and Yang, 2022; Zhang et al., 2017; Woodward et al., 2019). A coupling mechanism between MATSim and the PALM model system using vehicle positions rendered with MATSim as moving emission sources in a PALM-4U simulation is currently under development.

6. Code and data availability

The conversion tool described in this article can be found at `https://gitlab.palm-model.org/matsim/matsim_traffic_emmisions/-/tree/mosaik-2-01`, an open-source git repository hosted as part of the PALM model system and was run with the version captured in (Laudan, 2023a).

The MATSim setup can be found at `https://github.com/matsim-scenarios/matsim-berlin/releases/tag/mosaik-2-01` and was run with the *MosaikRunner.java* class (vsp-gleich et al., 2023).

The original PALM-4U setup can be found at `10.5281/zenodo.4153388` a data repository stored at the Zenodo project (Khan, 2020).

All input and output data related to this article can be found at `https://doi.org/10.14279/depositonce-18737`, a data repository hosted at Technische Universität Berlin (Laudan, 2023b)

7. Funding

This work was partially funded by the BMBF Bundesministerium für Bildung und Forschung [grant number 01LP1911C]

References

Agarwal, A., 2017. Mitigating negative transport externalities in industrialized and industrializing countries. URL: https://depositonce.tu-berlin.de/handle/11303/6266, doi:10.14279/depositonce-5825.

Agency, U.S.E.P., 2002. User's guide to MOBILE6. 0: Mobile source emission factor model.

Alvarez Lopez, P., Behrisch, M., Bieker-Walz, L., Erdmann, J., Flötteröd, Y.P., Hilbrich, R., Lücken, L., Rummel, J., Wagner, P., Wießner, E., 2018. Microscopic traffic simulation using SUMO, in: 2019 IEEE Intelligent Transportation Systems Conference (ITSC), IEEE. pp. 2575–2582. URL: https://elib.dlr.de/127994/, doi:10.1109/ITSC.2018.8569938.

André, M., Keller, M., Sjödin, Å., Gadrat, M., Mc Crae, I., 2008. The artemis european tools for estimating the pollutant emissions from road transport and their application in sweden and france, in: In Proceedings of the 17th International Conference Transport and Air Pollution. URL: https://citeseerx.ist.psu.edu/document?repid=rep1&type=pdf&doi=399e8ff96aad8c28ebf79e2414d869203f9c768b.

Batterman, S., Ganguly, R., Harbin, P., 2015. High resolution spatial and temporal mapping of traffic-related air pollutants. Int. J. Environ. Res. Public Health 12, 3646–3666. URL: http://dx.doi.org/10.3390/ijerph120403646, doi:10.3390/ijerph120403646.

Benson, P.E., 1992. A review of the development and application of the CALINE3 and 4 models. Atmospheric Environment. Part B. Urban Atmosphere 26, 379–390. URL: https://www.sciencedirect.com/science/article/pii/095712729290013I, doi:10.1016/0957-1272(92)90013-I.

Berkowicz, R., Hertel, O., Larsen, S.E., Soerensen, N.N., Nielsen, M., 1997. Modelling traffic pollution in streets. Technical Report. National Environmental Research Institute, Denmark. URL: https://www.osti.gov/etdeweb/biblio/438467.

Blocken, B., 2018. LES over RANS in building simulation for outdoor and indoor applications: A foregone conclusion? Build. Simul. 11, 821–870. URL: https://doi.org/10.1007/s12273-018-0459-3, doi:10.1007/s12273-018-0459-3.

Bresenham, J.E., 1965. Algorithm for computer control of a digital plotter. IBM Syst. J. 4, 25–30. URL: http://dx.doi.org/10.1147/sj.41.0025, doi:10.1147/sj.41.0025.

Cappiello, A., Chabini, I., Nam, E.K., Lue, A., Abou Zeid, M., 2002. A statistical model of vehicle emissions and fuel consumption, in: Proceedings. The IEEE 5th International Conference on Intelligent Transportation Systems, pp. 801–809. URL: http://dx.doi.org/10.1109/ITSC.2002.1041322, doi:10.1109/ITSC.2002.1041322.

Carruthers, D.J., Holroyd, R.J., Hunt, J.C.R., Weng, W.S., Robins, A.G., Apsley, D.D., Thompson, D.J., Smith, F.B., 1994. UK-ADMS: A new approach to modelling dispersion in the earth's atmospheric boundary layer. J. Wind Eng. Ind. Aerodyn. 52, 139–153. URL: https://www.sciencedirect.com/science/article/pii/0167610594900442, doi:10.1016/0167-6105(94)90044-2.

Ciarelli, G., Colette, A., Schucht, S., Beekmann, M., Andersson, C., Manders-Groot, A., Mircea, M., Tsyro, S., Fagerli, H., Ortiz, A.G., Adani, M., Briganti, G., Cappelletti, A., D'Isidoro, M., Cuvelier, C., Couvidat, F., Meleux, F., Bessagnet, B., 2019. Long-term health impact assessment of total PM2.5 in europe during the 1990–2015 period. Atmospheric Environment: X 3, 100032. URL: https://www.sciencedirect.com/science/article/pii/S2590162119300358, doi:10.1016/j.aeaoa.2019.100032.

Desa, U.N., 2018. World Urbanization Prospects 2018: Highlights. Technical Report. United Nations.

Diegmann, V., 2011. handbuch_immisluft_5_2.pdf. IVU Umwelt GmbH. URL: http://www.ivu-umwelt.de/upload/download/handbuecher/handbuch_immisluft_5_2.pdf.

Dons, E., Int Panis, L., Van Poppel, M., Theunis, J., Willems, H., Torfs, R., Wets, G., 2011. Impact of time–activity patterns on personal exposure to black carbon. Atmos. Environ. 45, 3594–3602. URL: https://www.sciencedirect.com/science/article/pii/S1352231011003359, doi:10.1016/j.atmosenv.2011.03.064.

DWD-Deutscher Wetter Dienst, . Climate data center. https://cdc.dwd.de/portal/202209231028/mapview. URL: https://cdc.dwd.de/portal/202209231028/mapview. accessed: 2024-1-2.

Ehrnsperger, L., Klemm, O., 2022. Air pollution in an urban street canyon: Novel insights from highly resolved traffic information and meteorology. Atmospheric Environment: X 13, 100151. URL: https://www.sciencedirect.com/science/article/pii/S2590162122000053, doi:10.1016/j.aeaoa.2022.100151.

EMEP/EEA, 2016. Air Pollutant Emission Inventory Guidebook 2016: Technical Guidance to Prepare National Emission Inventories. European Environment Agency. URL: https://play.google.com/store/books/details?id=q5qPswEACAAJ.

Epa, U.S., 2021. Overview of EPA's MOtor Vehicle Emission Simulator (MOVES3). U.S. Environmental Protection Agency. URL: https://nepis.epa.gov/Exe/ZyPDF.cgi?Dockey=P1011KV2.pdf.

European Environment Agency, 2020. Air Quality in Europe: 2020 Report. Publications Office of the European Union. URL: https://play.google.com/store/books/details?id=swtezgEACAAJ.

Forehead, H., Huynh, N., 2018. Review of modelling air pollution from traffic at street-level - the state of the science. Environ. Pollut. 241, 775–786. URL: http://dx.doi.org/10.1016/j.envpol.2018.06.019, doi:10.1016/j.envpol.2018.06.019.

Grumert, E., Ma, X., Tapani, A., 2015. Analysis of a cooperative variable speed limit system using microscopic traffic simulation. Transp. Res. Part C: Emerg. Technol. 52, 173–186. URL: https://www.sciencedirect.com/science/article/pii/S0968090X14003210, doi:10.1016/j.trc.2014.11.004.

Horni, A., Nagel, K., Axhausen, K.W., 2016. The Multi-Agent Transport Simulation Matsim. Ubiquity Press. URL: https://play.google.com/store/books/details?id=g91_DQEACAAJ, doi:10.5334/baw.

Hülsmann, F., Gerike, R., Kickhöfer, B., Nagel, K., Luz, R., 2011. Towards a multi-agent based modeling approach for air pollutants in urban regions Entwicklung eines Ansatzes zur multi-agentenbasierten Modellierung von Luftschadstoffemissionen in urbanen Regionen. In Conference on "Luftqualität an Straßen", pages 144–166, Bundesanstalt für Straßenwesen, FGSV Verlag GmbH. URL: https://svn.vsp.tu-berlin.de/repos/public-svn/publications/vspwp/2010/10-15/2011-01-05_emissionsTestRoadbast_accepted_BAST11.pdf.

Johnson, J.B., 2022. An introduction to atmospheric pollutant dispersion modelling. Environmental Sciences Proceedings 19, 18. URL: https://www.mdpi.com/2673-4931/19/1/18, doi:10.3390/ecas2022-12826.

José, R.S., Pérez, J.L., Morant, J.L., González, R.M., 2008. CFD and mesoscale air quality modelling integration: Web application for las palmas (canary islands, spain), in: Air Pollution Modeling and Its Application XIX, Springer Netherlands. pp. 37–45. URL: http://dx.doi.org/10.1007/978-1-4020-8453-9_4, doi:10.1007/978-1-4020-8453-9_4.

Khan, B., 2020. Input data for performing chemistry coupled PALM model system 6.0 simulations with different chemical mechanisms. URL: https://zenodo.org/record/4153388, doi:10.5281/zenodo.4153388.

Khan, B., Banzhaf, S., Chan, E.C., Forkel, R., Kanani-Sühring, F., Ketelsen, K., Kurppa, M., Maronga, B., Mauder, M., Raasch, S., Others, 2021. Development of an atmospheric chemistry model coupled to the PALM model system 6.0: implementation and first applications. Geoscientific Model Development 14, 1171–1193. URL: https://gmd.copernicus.org/articles/14/1171/2021/, doi:10.5194/gmd-14-1171-2021.

Kickhöfer, B., Hülsmann, F., Gerike, R., Nagel, K., 2013. Rising car user costs: comparing aggregated and geo-spatial impacts on travel demand and air pollutant emissions, in: Smart Transport Networks. Edward Elgar Publishing, pp. 180–207. URL: https://www.elgaronline.com/view/edcoll/9781782548324/9781782548324.00014.xml, doi:10.4337/9781782548331.00014.

Laudan, J., 2023a. MATSim traffic emission module for PALM. URL: https://zenodo.org/record/8319087, doi:10.5281/ZENODO.8319087.

Laudan, J., 2023b. Mosaik-2 simulation experiment. URL: https://depositonce.tu-berlin.de/items/bd40f70b-d194-49a2-a70c-8ec6db364c24, doi:10.14279/depositonce-18737.

Liang, M., Chao, Y., Tu, Y., Xu, T., 2023. Vehicle pollutant dispersion in the urban atmospheric environment: A review of mechanism, modeling, and application. Atmosphere 14, 279. URL: https://www.mdpi.com/2073-4433/14/2/279, doi:10.3390/atmos14020279.

Lim, S., Holliday, L., Barratt, B., Griffiths, C.J., Mudway, I.S., 2021. Assessing the exposure and hazard of diesel exhaust in professional drivers: a review of the current state of knowledge. Air Qual. Atmos. Health 14, 1681–1695. URL: https://doi.org/10.1007/s11869-021-01048-0, doi:10.1007/s11869-021-01048-0.

Ma, X., Lei, W., Andréasson, I., Chen, H., 2012. An evaluation of microscopic emission models for traffic pollution simulation using on-board measurement. Environ. Model. Assess. 17, 375–387. URL: https://doi.org/10.1007/s10666-011-9296-9, doi:10.1007/s10666-011-9296-9.

Mądziel, M., 2023. Vehicle emission models and traffic simulators: A review. Energies 16, 3941. URL: https://www.mdpi.com/1996-1073/16/9/3941, doi:10.3390/en16093941.

Maronga, B., Banzhaf, S., Burmeister, C., Esch, T., Forkel, R., Fröhlich, D., Fuka, V., Gehrke, K.F., Geletič, J., Giersch, S., Gronemeier, T., Groß, G., Heldens, W., Hellsten, A., Hoffmann, F., Inagaki, A., Kadasch, E., Kanani-Sühring, F., Ketelsen, K., Khan, B.A., Knigge, C., Knoop, H., Krč, P., Kurppa, M., Maamari, H., Matzarakis, A., Mauder, M., Pallasch, M., Pavlik, D., Pfafferott, J., Resler, J., Rissmann, S., Russo, E., Salim, M., Schrempf, M., Schwenkel, J., Seckmeyer, G., Schubert, S., Sühring, M., von Tils, R., Vollmer, L., Ward, S., Witha, B., Wurps, H., Zeidler, J., Raasch, S., 2020. Overview of the PALM model system 6.0. Geosci. Model Dev. 13, 1335–1372. URL: https://gmd.copernicus.org/articles/13/1335/2020/, doi:10.5194/gmd-13-1335-2020.

Maronga, B., Gross, G., Raasch, S., Banzhaf, S., Forkel, R., Heldens, W., Kanani-Sühring, F., Matzarakis, A., Mauder, M., Pavlik, D., Pfafferott, J., Schubert, S., Seckmeyer, G., Sieker, H., Winderlich, K., 2019. Development of a new urban climate model based on the model PALM – project overview, planned work, and first achievements. Meteorol. Z. 28, 105–119. URL: http://www.schweizerbart.de/papers/metz/detail/28/90483/Development_of_a_new_urban_climate_model_based_on_?af=crossref, doi:10.1127/metz/2019/0909.

McConnell, R., Islam, T., Shankardass, K., Jerrett, M., Lurmann, F., Gilliland, F., Gauderman, J., Avol, E., Künzli, N., Yao, L., Peters, J., Berhane, K., 2010. Childhood incident asthma and traffic-related air pollution at home and school. Environ. Health Perspect. 118, 1021–1026. URL: http://dx.doi.org/10.1289/ehp.0901232, doi:10.1289/ehp.0901232.

Notter, B., Keller, M., Althaus, H.J., Cox, B., Knörr, W., Heidt, C., Biemann, K., Räder, D., Jamet, M., 2019. Handbuch Emissionsfaktoren des Strassenverkehrs. Technical Report 4.1. INFRAS. Sennweg 2, 3012 Bern, Switzerland. URL: https://www.hbefa.net/.

Ntziachristos, L., 2000. COPERT III Computer Programme to Calculate Emissions from Road Transport: Methodology and Emission Factors (Version 2.1). European Environment Agency. URL: https://play.google.com/store/books/details?id=4FuuGwAACAAJ.

Qi, Y.g., Teng, H.h., Yu, L., 2004. Microscale emission models incorporating acceleration and deceleration. J. Transp. Eng. 130, 348–359. URL: http://dx.doi.org/10.1061/(ASCE)0733-947X(2004)130:3(348), doi:10.1061/(asce)0733-947x(2004)130:3(348).

Rakha, H., Ahn, K., Trani, A., 2004. Development of VT-Micro model for estimating hot stabilized light duty vehicle and truck emissions. Transp. Res. Part D: Trans. Environ. 9, 49–74. URL: https://www.sciencedirect.com/science/article/pii/S1361920903000543, doi:10.1016/S1361-9209(03)00054-3.

San José, R., Pérez, J.L., Gonzalez-Barras, R.M., 2021. Assessment of mesoscale and microscale simulations of a NO2 episode supported by traffic modelling at microscopic level. Sci. Total Environ. 752, 141992. URL: http://dx.doi.org/10.1016/j.scitotenv.2020.141992, doi:10.1016/j.scitotenv.2020.141992.

Sanchez, B., Santiago, J.L., Martilli, A., Martin, F., Borge, R., Quaassdorff, C., de la Paz, D., 2017. Modelling NOX concentrations through CFD-RANS in an urban hot-spot using high resolution traffic emissions and meteorology from a mesoscale model. Atmos. Environ. 163, 155–165. URL: https://www.sciencedirect.com/science/article/pii/S1352231017303230, doi:10.1016/j.atmosenv.2017.05.022.

von Schneidemesser, E., Sibiya, B., Caseiro, A., Butler, T., Lawrence, M.G., Leitao, J., Lupascu, A., Salvador, P., 2021. Learning from the COVID-19 lockdown in berlin: Observations and modelling to support understanding policies to reduce NO2. Atmos Environ X 12, 100122. URL: http://dx.doi.org/10.1016/j.aeaoa.2021.100122, doi:10.1016/j.aeaoa.2021.100122.

Schulz, H., Karrasch, S., Bölke, G., Cyrys, J., Hornberg, C., Pickford, R., Schneider, A., Witt, C., Hoffmann, B., 2018. Atmen. DGfPuB eV Deutsche Gesellschaft für PneumologieundBeatmungsmedizine. V. , Berlin URL: https://pneumologie.de/fileadmin/DGP_Luftschadstoffe_Positionspapier_20190129.pdf.

Schümann, L., Grunow, K., Kaupp, H., Clemen, S., Kerschbaumer, A., Rauterberg-Wulff, A., 2021. Luftgütemessdaten Jahresbericht 2021. Technical Report. Senatsverwaltung für Umwelt, Mobilität, Verbraucher- und Klimaschutz.

Scora, G., Barth, M., 2006. Comprehensive modal emissions model (cmem), version 3.01. User guide. Centre for environmental research and technology. University of California, Riverside 1070, 1580. URL: https://www.cert.ucr.edu/sites/default/files/2019-07/CMEM_User_Guide_v3.01d.pdf.

Senatsverwaltung für Mobilität, Verkehr, Klimaschutz und Umwelt, . Berliner luftgütemessnetz. https://luftdaten.berlin.de/station/overview/active. URL: https://luftdaten.berlin.de/station/overview/active. accessed: 2024-1-2.

Smit, R., Smokers, R., Rabé, E., 2007. A new modelling approach for road traffic emissions: VERSIT+. Transp. Res. Part D: Trans. Environ. 12, 414–422. URL: https://www.sciencedirect.com/science/article/pii/S1361920907000521, doi:10.1016/j.trd.2007.05.001.

Snyder, M.G., Venkatram, A., Heist, D.K., Perry, S.G., Petersen, W.B., Isakov, V., 2013. RLINE: A line source dispersion model for near-surface releases. Atmos. Environ. 77, 748–756. URL: https://www.sciencedirect.com/science/article/pii/S1352231013004470, doi:10.1016/j.atmosenv.2013.05.074.

Tominaga, Y., Stathopoulos, T., 2016. Ten questions concerning modeling of near-field pollutant dispersion in the built environment. Build. Environ. 105, 390–402. URL: https://www.sciencedirect.com/science/article/pii/S0360132316302347, doi:10.1016/j.buildenv.2016.06.027.

UC2, 2023. BMBF-Fördermaßnahme stadtklima im wandel. http://uc2-program.org/. URL: http://uc2-program.org/. accessed: 2023-1-9.

Vardoulakis, S., Fisher, B.E.A., Pericleous, K., Gonzalez-Flesca, N., 2003. Modelling air quality in street canyons: a review. Atmos. Environ. 37, 155–182. URL: https://www.sciencedirect.com/science/article/pii/S1352231002008579, doi:10.1016/S1352-2310(02)00857-9.

vsp-gleich, kainagel, Rehmann, J., tschlenther, Martins-Turner, K., dziemke, Hugo-CM, Marc, Maciejewski, M., Zilske, M., rakow, aravindsasi, Laudan, J., Ewert, R., Müller, S., Marcel, 2023. matsim-scenarios/matsim-berlin: Mosaik-2-01. URL: https://zenodo.org/record/8319022, doi:10.5281/zenodo.8319022.

Wendt, J., 2008. Computational Fluid Dynamics: An Introduction. Springer Science & Business Media. URL: https://play.google.com/store/books/details?id=IIUkqI-HNbQC.

Woodward, H., Stettler, M., Pavlidis, D., Aristodemou, E., ApSimon, H., Pain, C., 2019. A large eddy simulation of the dispersion of traffic emissions by moving vehicles at an intersection. Atmos. Environ. 215, 116891. URL: https://www.sciencedirect.com/science/article/pii/S1352231019305308, doi:10.1016/j.atmosenv.2019.116891.

Zhang, Y., Gu, Z., Yu, C.W., 2017. Large eddy simulation of vehicle induced turbulence in an urban street canyon with a new dynamically vehicle-tracking scheme. Aerosol Air Qual. Res. 17, 865–874. URL: https://aaqr.org/articles/aaqr-16-05-oa-0204, doi:10.4209/aaqr.2016.05.0204.

Zheng, X., Yang, J., 2022. Impact of moving traffic on pollutant transport in street canyons under perpendicular winds: A CFD analysis using large-eddy simulations. Sustainable Cities and Society 82, 103911. URL: https://www.sciencedirect.com/science/article/pii/S2210670722002335, doi:10.1016/j.scs.2022.103911.

Ziemke, D., Kaddoura, I., Nagel, K., 2019. The MATSim open berlin scenario: A multimodal agent-based transport simulation scenario based on synthetic demand modeling and open data. Procedia Comput. Sci. 151, 870–877. URL: https://www.sciencedirect.com/science/article/pii/S1877050919305848, doi:10.1016/j.procs.2019.04.120.